ELSEVIER
Journal of Nuclear Materials 290–293 (2001) 423–427
journal of nuclear materials
www.elsevier.nl/locate/jnucmat

Modeling of wall recycling effects on the global particle balance in magnetic fusion devices

Y. Hirooka *, S. Masuzaki, H. Suzuki, T. Kenmotsu, T. Kawamura

National Institute for Fusion Science, 322-6 Oroshi, Toki, Gifu-Pref, 509-5292, Japan

Abstract

A zero-dimensional particle balance model has been developed to compute hydrogen inventories in the four major reservoirs; core plasma, scraped-off layer (SOL), gas region, and wall of a magnetic fusion reactor system. This model takes as input separately calculated hydrogen reemission and reflection coefficients. Model applications have successfully reproduced the core plasma transient behavior with and without density decay observed in the large helical device (LHD). Particle balance modeling has also been done for a hypothetical steady-state reactor employing carbon as the plasma-facing material. Results indicate that codeposition-induced wall pumping is quite effective in controlling the core density although, on the other hand, the tritium inventory concerns environmental safety.

Keywords: LHD; Hydrogen recycling; Modelling; Particle control; Wall pumping; Particle balance

1. Introduction

To demonstrate magnetic fusion as a viable energy source, one has to develop a knowledge basis and capabilities of sustaining ignited plasmas at steady state. Currently operated in Japan for this purpose are LHD and TRIAM-1M. Also, ITER has motivated international efforts on steady-state reactor studies.

Among other technical issues, particle control is particularly important because it affects a wide range of aspects of reactor operation, including the core plasma confinement, in-vessel components lifetime, fuel economy and even environmental safety associated with tritium management. Closely related to these, plasma–wall interactions play a crucial role in determining particles' whereabouts in a reactor system. Fuel particles escaping from the plasma are implanted into plasma-facing materials but they will be released with a characteristic time constant. In addition, materials erosion and redeposition can affect particle balance via hydrogen codeposition. This fuel recycling is a key to understand the global particle balance in a reactor not only during the start-up transient but also during the steady-state operation.

In an attempt to understand the global particle balance, numerous experiments coupled with modeling have recently been conducted worldwide, using major facilities: JT-60 [1], DIII-D [2], Tore Supra [3], JET [4,5]. Some of these studies deal with only two reservoirs of particles: plasma and wall [5] or segmented walls [2,3] whereas others assume another reservoir, either SOL [4] or pump [1,2].

In this study, for more advanced analysis of the core density behavior in LHD [6,7] and future steady-state reactors, four-reservoir modeling has been performed, together with rather detailed hydrogen recycling modeling. Also, effects of atomic and molecular reactions such as charge exchange and gas ionization are taken into account in this modeling.

2. Particle balance modeling

2.1. Hydrogen reemission and reflection

The formalism employed here to describe hydrogen reemission is essentially the same as the one for the DIFFUSE-code [8]. However, the original formalism has been modified in order that time-varying plasma–wall

* Corresponding author. Tel.: +81-572 58 2256; fax: +81-572 58 2628.

E-mail address: hirooka@nifs.ac.jp (Y. Hirooka).

0022-3115/01/$ - see front matter
PII: S0022-3115(00)00640-1

interaction conditions can be incorporated. The mathematical expressions of the present model are as follows:

$$\frac{\partial C_m(x,t)}{\partial t} = D\{T(t)\}\frac{\partial^2 C_m(x,t)}{\partial x^2} - \frac{\partial C_t(x,t)}{\partial t} + G(x,t), \quad (1)$$

$$\frac{\partial C_t(x,t)}{\partial t} = D\{T(t)\}\{C_T^0(x) - n_t C_t(x,t)\}/\lambda^2 - C_t(x,t)v_0 \times \exp(-Q_t/kT(t)), \quad (2)$$

where x is the thickness position, t is the time, D is the diffusion coefficient, T is the temperature, C_m is the mobile atom concentration, G is the source term, C_T^0 is the initial trapping site concentration, C_t is the tapped atom concentration, n_t is the number of hydrogen atoms that can share each trapping site, λ is the detrapping jump distance taken as the lattice constant, v_0 is the jumping frequency taken as 10^{13} [8] and Q_t is the activation energy for detrapping. Notice that D, T and G are treated as functions of time. For simplicity, n_t is assumed to be unity. The particle reflection coefficient and implantation profile are calculated, using the TRIM.SP code [9].

Assuming that hydrogen reemission from the front surface is controlled by recombinative desorption and inward transport is limited by diffusion, the boundary conditions for solving equations (1) and (2) are expressed as follows:

$$D\{T(t)\}\frac{\partial C_m(x_s,t)}{\partial t} = K_r C_m(x_s,t)^2, \quad C_m(x_{max},t) = 0, \quad (3)$$

where K_r is the surface recombination coefficient, and x_s and x_{max} correspond to the front surface and the diffusion thickness, respectively.

2.2. Global particle balance modeling

In 1998, considerable attention was brought to the observation in LHD that the core plasma density decays, even as external fueling continues, during the plasma heating by neutral beam injection (NBI) [6,7]. About a decade ago, similar density decay was observed in JT-60 [1]. These observations may be explained as the result of: (1) wall pumping [1,6]; (2) a decrease in fueling efficiency [7]; and (3) degradation of particle confinement [10]. The present work is intended to investigate the role of wall recycling in determining core density behavior.

Developed for this purpose is a zero-dimensional particle balance model. Using hydrogen reemission and reflection coefficients, this model calculates particle inventories in the four reservoirs: (1) core; (2) SOL; (3) gas region and (4) wall. Hydrogen inventories in these reservoirs, denoted by N_{core}, N_{SOL}, N_{gas}, and N_{wall}, can be obtained by solving the following set of differential equations:

$$\frac{dN_{core}}{dt} = -\frac{N_{core}}{\tau_{core}} + \alpha\frac{\langle\sigma v\rangle_{cx}}{2V_{gas}}N_{gas}N_{SOL} + \left(\frac{N_{SOL}}{\tau_{SOL}} + \alpha\frac{\langle\sigma v\rangle_{cx}}{2V_{gas}}N_{gas}N_{SOL}\right) \times (R_{ef}{}^{ref}f_{wall} + R_e{}^{re}f_{core}) + f_{core}\Phi_{ext}, \quad (4)$$

$$\frac{dN_{SOL}}{dt} = -\frac{N_{SOL}}{\tau_{SOL}} + \frac{N_{core}}{\tau_{core}} - \alpha\frac{\langle\sigma v\rangle_{cx}}{V_{gas}}N_{gas}N_{SOL} + \beta\frac{\langle\sigma v\rangle_{ion}}{V_{SOL}}N_{gas}N_{SOL} + \left(\frac{N_{SOL}}{\tau_{SOL}} + \alpha\frac{\langle\sigma v\rangle_{cx}}{2V_{gas}}N_{gas}N_{SOL}\right) \times \{R_e{}^{re}f_{SOL} + R_{ef}(1 - {}^{ref}f_{wall})\} + f_{SOL}\Phi_{ext}, \quad (5)$$

$$\frac{dN_{gas}}{dt} = -S_pN_{gas} - \beta\frac{\langle\sigma v\rangle_{ion}}{V_{SOL}}N_{gas}N_{SOL} + \left(\frac{N_{SOL}}{\tau_{SOL}} + \alpha\frac{\langle\sigma v\rangle_{cx}}{2V_{gas}}N_{gas}N_{SOL}\right) \times \{(R_e(1 - {}^{re}f_{SOL} - {}^{re}f_{core}) - \gamma Y_{sput}\} + (1 - f_{core} - f_{SOL})\Phi_{ext}, \quad (6)$$

$$\frac{dN_{wall}}{dt} = \left(\frac{N_{SOL}}{\tau_{SOL}} + \alpha\frac{\langle\sigma v\rangle_{cx}}{2V_{gas}}N_{gas}N_{SOL}\right)(1 - R_e - R_{ef} + \gamma Y_s) \quad (7)$$

and the initial conditions are set as follows:

$$N_{core} = N_{SOL} = N_{wall} = 0, \quad N_{gas} = N_0(\text{at } t = 0), \quad (8)$$

where τ_{core} and τ_{SOL} are the plasma confinement times in core and SOL, respectively; $\langle\sigma v\rangle_{cx}$ and $\langle\sigma v\rangle_{ion}$ the rate coefficients for the reactions: $H + H^+ \to H^+ + H$ and $H_2 + e^- \to H_2^+ + 2e^-$ [11]; α and β are the adjusting parameters (usually $\alpha/\beta = 1$), respectively; R_{ef} and R_e are the reflection and reemission coefficients, respectively; V_{SOL} and V_{gas} are the volumes of SOL and Gas, respectively; f_{core}, and f_{SOL} are the fueling efficiencies by external gas puffing into core and SOL, respectively; ${}^{re}f_{core}$ and ${}^{re}f_{SOL}$ are the fueling efficiencies by wall-reemitted gas into core and SOL, respectively; ${}^{ref}f_{core}$ is the fueling efficiency by wall-reflected particles into core; ϕ_{ext} is the gas puffing rate; S_p is the pumping speed; γ is the hydrogen codeposition efficiency; Y_s is the sputtering yield; and N_0 is the initial inventory in gas.

It is *extremely important* to note that for a closed divertor device such as DIII-D with a fully toroidal pumping slot, particle exhaust is directed into it by the intrinsic plasma flow. Due to the compression effect [1], wall-recycled gas will not efficiently re-fuel the core plasma. In contrast, for an open divertor device, particle removal needs to be done by pumping wall-recycled gas. On its way to pumping ducts, however, wall-recycled gas tends to re-fuel the core and SOL plasmas. Therefore, it is essential that the Gas region and its effects be incorporated in the particle balance modeling for LHD.

3. Model applications and discussion

3.1. Density decay during NBI-heating in LHD

During the second experimental campaign, diverted hydrogen plasma operation was performed in LHD with the external fueling done by gas puffing. The typical operational scenario was such that plasma breakdown was done by electron-cyclotron heating (ECH) with the power up to 300 kW and subsequently heating was taken over by NBI with the power up to 3 MW. Generally, as soon as NBI-heating kicks in, the divertor temperature rises with a characteristic time constant, apparently related to the energy confinement time of the order of 100 ms. Core density decay was observed during NBI-heating, as shown in Fig. 1, even as gas puffing continues.

Interestingly, the statistics on LHD data indicates that density decay occurs only when the edge temperature at the last closed flux surface exceeds a certain level around 170 eV, and the corresponding divertor temperature is around 25 eV [6]. The divertor temperature during ECH-breakdown is usually around 5 eV. The core density evolution without decay is also shown in Fig. 1. Although the water-cooled 316 stainless steel vessel was directly exposed to the divertor plasma, due to the moderate power flux, the surface temperature was observed to rise up to around 50°C [12].

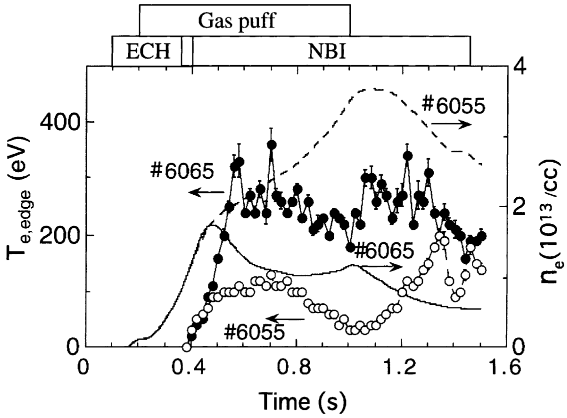

Fig. 1. The core plasma behaviour with and without density decay during NBI-heating, observed in LHD (after Masuzaki et al. [6]). Here, shot #6055 shows density decay. The ECH, NBI and gas puff indicators are for shot #6055. Those for Shot #6065 are not shown but similar to #6055. The electron temperature shown here is the one measured at the last closed flux surface (not in the divertor region).

Particle balance modeling has been performed, simulating these conditions in LHD. A wave form is employed to calculate the recycling coefficients in such a way that at $t = 0$ s the wall flux exponentially ramps up to a flat-top of 2×10^{18} 1/cm^2/s and at $t = 1$ s ramps down as external fueling stops, where the time constants for these ramps are set equal to the particle confinement time. One can then find the effect of it if wall recycling is affected by the divertor temperature change. The ion bombarding energy, E, is determined from the relation:

Table 1
Input parameters for the particle balance modeling

	LHD (1998)	Reactor
Core plasma volume	30 000 l	631 000 l
Core confinement time: τ_{core}	0.1 s (0.2 s^a)	1 s (1.5 s^a)
SOL plasma volume: V_{SOL}	10 000 l	32 000 l
SOL confinement time: τ_{SOL}	0.001 s (0.002 s^a)	0.001 s (0.002 s^a)
Gas region volume: V_{gas}	180 000 l	←
Divertor plasma temperature	25 eV (5 eV^a)	←
Divertor material (temperature)	316 SS (50°C)	Carbon (500°C)
Hydrogen diffusivity [14]	$3.8 \times 10^{-3}\ \exp(-0.56\ [eV]/kT)$	$7.0 \times 10^{-3}\ \exp(-0.5\ [eV]/kT)$
Surface recombination coefficient[14]	$2.1 \times 10^{-18}\ \exp(-0.34\ [eV]/kT)/\sqrt{T}$	$8.5 \times 10^{-17}\ \exp(-0.45\ [eV]/kT)/\sqrt{T}$
Pumping speed: S_p	66 700 l/s	100 000 l/s
External fueling: ϕ_{ext}	20 Torr l/s	← (1 Torr l/s^b)
Fueling efficiencies^c		
Core fueling by gas: $f_{core} = {}^{re}f_{core}$	0.1 (0.7^a)	←
SOL fueling by gas: $f_{SOL} = {}^{re}f_{SOL}$	0.7 (0.1^a)	←
Core fueling by fast particles: ${}^{ref}f_{core}$	0.3	←
SOL fueling by fast particles: $1 - {}^{ref}f_{core}$	0.7	←

[a] Values before NBI-heating.
[b] External fueling rate in the case study without hydrogen co-deposition.
[c] Calculated assuming the SOL thickness is 5 cm and the density is 5×10^{12} 1/cm^3.

$E = 6\ kT_e$ [13], assuming that $T_e = T_i$, where k is the Boltzmann constant, T_e and T_i are the electron and ion temperatures, respectively. The bombarding angle is set at 45° with respect of the surface. The hydrogen trapping site concentration and detrapping energy in 316 stainless steel are taken as 1 at.% and 0.22 eV, respectively [14]. Other input parameters are summarized in Table 1.

Model calculation results are shown in Fig. 2. For comparison, two sets of runs have been performed at the NBI-heated divertor plasma temperatures of 25 and 15 eV. Notice that in these two cases ion implantation profiles are clearly different in peak separation and depth broadening (Figs. 2(a) and (b)). For both cases, however, the total recycling coefficient (reemission plus reflection) exhibits complex behavior (Figs. 2(c) and (d)). The total recycling coefficient rises at first but then falls, as shown in Fig. 2(c), while the implantation profile slides in depth along with NBI-heating. Halfway up to saturation with the re-established profile, at $t = 1$ s, the recycling coefficient falls due to the termination of external fueling. Along with this, the core and SOL densities exhibit characteristic decay (Fig. 2(e)). In contrast, as shown in Fig. 2(d), the recycling coefficient experiences a temporary plateau which, however, is followed by another rise to exceed unity, leading to an increase in core density, apparently an overflow due to the limited pumping speed (Fig. 2(f)).

As is always the case, it is impossible to estimate all the input parameters for modeling of this kind. Given the uncertainty, though it is possible, we choose not to present here the 'best fit' by adjusting input parameters. Nonetheless, as shown in Figs. 2(d) and (e), model calculations have successfully reproduced all key features of the core plasma behavior with and without density decay observed in LHD.

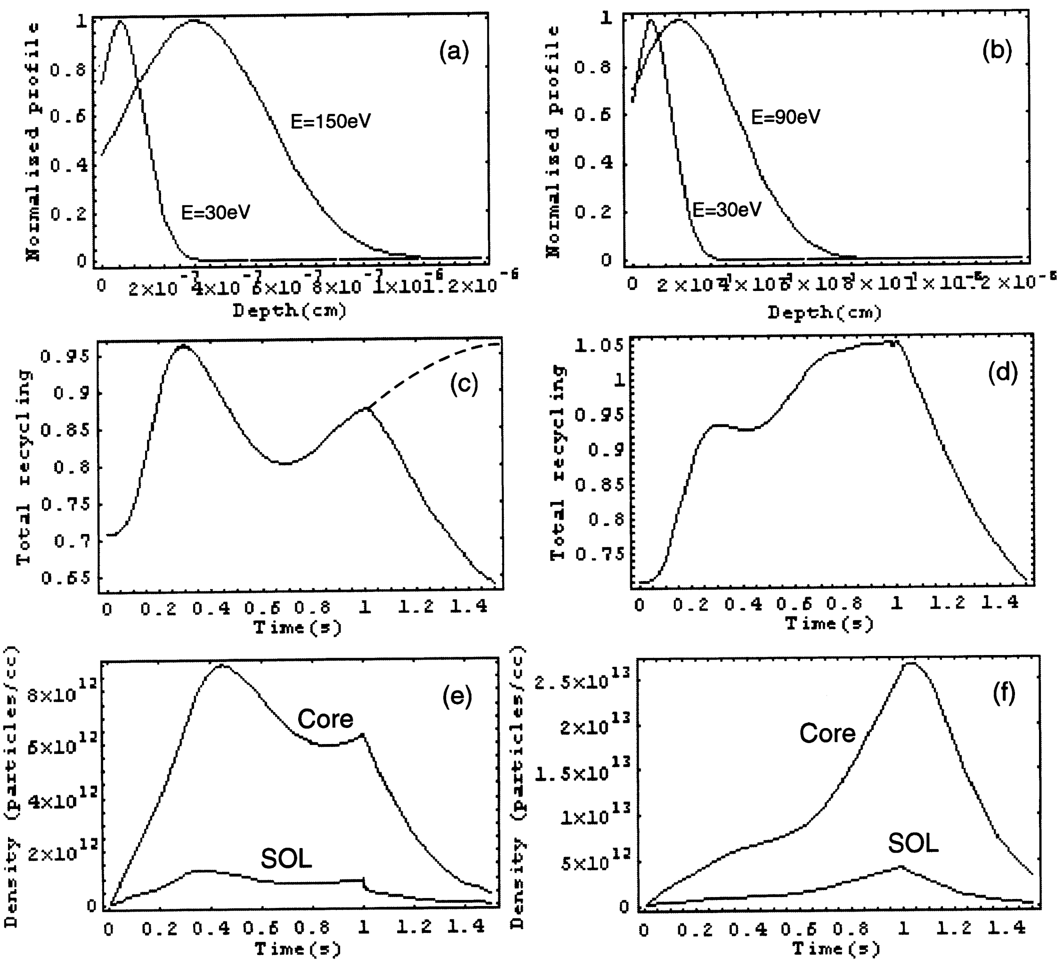

Fig. 2. Results of particle balance modeling on LHD: (a) and (b) are hydrogen implanation profiles into stainless steel, simulating NBI-heated divertor plasma temperatures of 25 and 15 eV, respectively; (c) and (d) are computed total recycling coefficients (reemission plus reflection); (e) and (f) are core and SOL plasma densities with and without characteristic decay, respectively. The dashed line in (c) indicates a hypothetical case with continued fueling.

3.2. Wall recycling and density control in a reactor-scale device

In this section wall recycling effects on the core density control in a reactor-scale device is analyzed using the model validated with the LHD case study. A semi-closed divertor configuration is employed, so that α/β is set at 0.1 to reflect a restricted fueling effect by wall-recycled gas. Long-pulse operation with the duration of 1000 s is simulated. No burn effect to consume deuterium and tritium is assumed for simplicity. A carbon divertor plate is employed and the operation temperature is assumed to be 500°C. Other input parameters are summarized in Table 1.

Shown in Fig. 3 are particle inventories in the four reservoirs in two cases with and without hydrogen codeposition. Clearly, without hydrogen codeposition (see Fig. 3(a)), the core density is not controlled so well as to establish a steady state even at a reduced fueling rate of 1 Torr l/s and a large pumping speed of 100,000 l/s. In contrast, assuming hydrogen codeposition with $\gamma = 0.2$ and $Y_s = 0.05$ [15] (Fig. 3(b)), the core density is well controlled for the long-pulse steady state even at a high fueling rate of 20 Torr l/s. Importantly, the wall pumping effect: $\gamma Y_s = 0.01$ results in the total recycling coefficient of 0.99 in Eq. (7). In exchange, however, the total inventory reaches the order of 10^{24} D+T atoms over 1000 s, a serious safety hazard. Meanwhile, inward diffusion due to the high-temperature operation builds up an additional inventory of the order of 10^{22} D+T atoms, which, however, is a minor contribution to the total inventory.

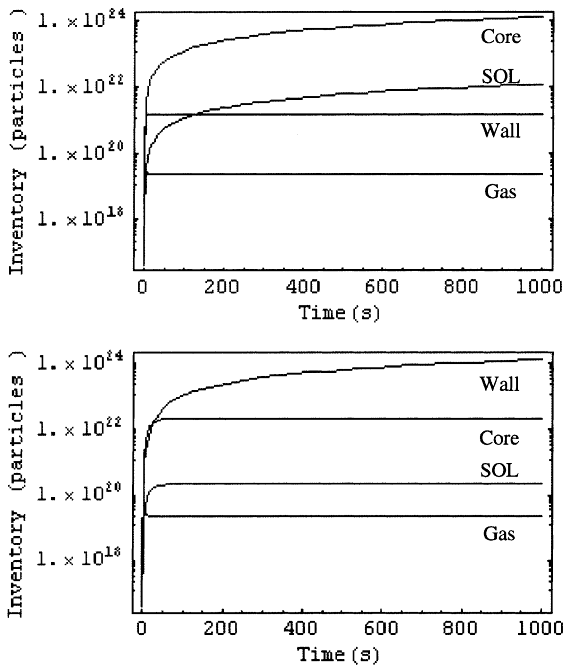

Fig. 3. Global particle balance simulation for a reactor-scale device: (a) without wall pumping; and (b) with wall pumping due to hydrogen codeposition at the rate, resulting in a 99% total wall recycling coefficient (see Eq. (7)).

4. Conclusion

Motivated by the core density decay observed in LHD, a zero-dimensional, four-reservoir particle balance model, coupled with hydrogen recycling calculations, has been developed. The model has successfully reproduced the characteristic density decay behavior. Results indicate that the implantation profile shifting in depth during NBI-heating apparently plays an important role in determining the recycling coefficient.

From the model application on a reactor-scale device, wall pumping due to hydrogen codeposition even at a moderate rate has been found to be far more effective in controlling the core density than employing a gigantic pumping system. For steady-state fusion reactors, therefore, reduced recycling is highly desirable *from the density control point of view* although it may require a yet-to-be explored wall concept.

References

[1] H. Nakamura et al., Nucl. Fus. 28 (1988) 43.
[2] P. Mioduszwski, in: Hydrogen Recycling and Wall Equilibration in Long-pulse Operation, presented at 10th Toki Conference, 22–26 January, 2000, Toki.
[3] M. Sugihara et al., J. Nucl. Mater. 266–269 (1999) 691.
[4] J. Ehrenberg, J. Nucl. Mater. 162–164 (1989) 63.
[5] T.T.C. Jones et al., J. Nucl. Mater. 162–164 (1989) 503.
[6] S. Masuzaki et al., in: Proceedings of the 26th EPS Conference on Contributions Fusion and Plasma Physics, vol. 23J, Maastricht, 14–18 June 1999, ECA, 1999, p. 1345.
[7] S. Morita et al., in: Proceedings of the 26th EPS Conference on Contributions Fusion and Plasma Physics, p. 1321.
[8] M.I. Baskes, Sadia Report 'DIFFUSE 83' SAND 83-8231.
[9] J.P. Biersack, W. Eckstein, Appl. Phys. A34 (1984) 73.
[10] JT-60 Team, in: Proceedings of the 11th IAEA International Conference on Plasma Physics and Contributions Fusion Research, vol. 1, 1987, p. 89.
[11] R.K. Janev et al., Elementary Processes in Hydrogen–Helium Plasmas, Springer, Berlin, 1987.
[12] S. Masuzaki, unpublished data.
[13] M.F.A. Harrison, in: R.K. Janev, H.W. Drawin, (Eds.), Atomic and Plasma–Material Interaction Processes in Controlled Thermonuclear Fusion, Elsevier, Amsterdam, 1993, p. 285.
[14] W. Möller, J. Roth, in: D.E. Post, R. Behrisch (Eds.), Physics of Plasma–Wall Interactions in Controlled Fusion, vol. 131, Plenum Press, New York, NATO ASI Series, 1984, p. 439.
[15] D.M. Goebel et al., Nucl. Fus. 28 (1988) 1041.